

# Non-monotonic responses of Atlantic Meridional Overturning Circulation to Antarctic meltwater forcing

Yechul Shin<sup>1</sup>, Xin Geng<sup>2</sup>, Ji-Hoon Oh<sup>3</sup>, Kyung Min Noh<sup>4</sup>, Emilia Kyung Jin<sup>5</sup>, and Jong-Seong Kug<sup>4</sup>

<sup>1</sup>Pohang University of Science and Technology

<sup>2</sup>Nanjing University of Information Science & Technology

<sup>3</sup>Pohang University of Science and Technology (POSTECH)

<sup>4</sup>POSTECH

<sup>5</sup>Korea Polar Research Institute

November 5, 2023

## Abstract

Antarctic meltwater discharge has been largely emphasized for its potential role in climate change mitigation, not only by reducing global warming, but also by stabilizing the Atlantic Meridional Overturning Circulation (AMOC). Despite the tremendous impact of the AMOC on the climate system, its temporal evolution to the meltwater remains poorly understood. In this study, we conduct idealized experiments to investigate the response of AMOC to Antarctic meltwater and discover a non-monotonic response of AMOC to the meltwater-induced cooling. Cold ocean surface caused by meltwater spread throughout the globe and eventually strengthened the AMOC. However, in the early stages, the tropical temperature response could stimulate the Rossby wave teleconnection, modulating atmospheric circulation in the North Atlantic, and weakening convection and even the AMOC. This counterintuitive evolution implies a potential destabilizing effect of Antarctic meltwater, and thus highlights the importance of the atmospheric dynamics in the interaction between the two poles.

## Hosted file

977945\_0\_art\_file\_11535226\_s3h7d7.docx available at <https://authorea.com/users/695875/articles/684378-non-monotonic-responses-of-atlantic-meridional-overturning-circulation-to-antarctic-meltwater-forcing>



1  
2 **Non-monotonic responses of Atlantic Meridional Overturning**  
3 **Circulation to Antarctic meltwater forcing**

4  
5 Yechul Shin<sup>1</sup>, Xin Geng<sup>1,2</sup>, Ji-Hoon Oh<sup>1</sup>, Kyung-Min Noh<sup>1</sup>, Emilia Kyung Jin<sup>3</sup>,  
6 and Jong-Seong Kug<sup>1\*</sup>

7  
8 <sup>1</sup>Division of Environmental Science and Engineering, Pohang University of Science and  
9 Technology (POSTECH), Pohang, Republic of Korea

10 <sup>2</sup>CIC-FEMD/ILCEC, Key Laboratory of Meteorological Disaster of Ministry of Education  
11 (KLME), Nanjing University of Information Science and Technology, Nanjing, China.

12 <sup>3</sup>Institute Korea Polar Research Institute (KOPRI), Incheon, Republic of Korea

13  
14 \*Corresponding author: Jong-Seong Kug ([jskug1@gmail.com](mailto:jskug1@gmail.com))

15 **Key Points:**

- 16
- 17 • The response of the AMOC to perennial meltwater-induced cooling varies, with the  
18 time scale determining its weakening or strengthening
  - 19 • Before the cooling spreads out the Atlantic, tropical atmospheric teleconnection could  
20 weaken the Greenland ocean convection
  - 21 • The non-monotonic response implies the importance of the atmospheric  
teleconnection to regulate polar climate

22 **Abstract**

23 Antarctic meltwater discharge has been largely emphasized for its potential role in  
24 climate change mitigation, not only by reducing global warming, but also by stabilizing the  
25 Atlantic Meridional Overturning Circulation (AMOC). Despite the tremendous impact of the  
26 AMOC on the climate system, its temporal evolution to the meltwater remains poorly  
27 understood. In this study, we conduct idealized experiments to investigate the response of  
28 AMOC to Antarctic meltwater and discover a non-monotonic response of AMOC to the  
29 meltwater-induced cooling. Cold ocean surface caused by meltwater spread throughout the  
30 globe and eventually strengthened the AMOC. However, in the early stages, the tropical  
31 temperature response could stimulate the Rossby wave teleconnection, modulating  
32 atmospheric circulation in the North Atlantic, and weakening convection and even the  
33 AMOC. This counterintuitive evolution implies a potential destabilizing effect of Antarctic  
34 meltwater, and thus highlights the importance of the atmospheric dynamics in the interaction  
35 between the two poles.

36

37 **Plain Language Summary**

38 The climate system is made up of interactions between different subsystems, so regional  
39 climate changes can have global effects. The freshwater discharge from Antarctica would  
40 increase in the future, resulting in regional cooling. Atmospheric and oceanic dynamics  
41 extend this local effect to the globe, reducing global surface temperature and strengthening  
42 the large-scale ocean circulation in the Atlantic, the Atlantic Meridional Overturning  
43 Circulation (AMOC). These mitigating effects naturally put the spotlight on Antarctic  
44 meltwater. However, our study shows that the mitigation effect depends on the time scale.  
45 Although the global mean temperature is always reduced, the AMOC surprisingly slows  
46 down as a first response to Antarctic meltwater driven by fast atmospheric teleconnection.  
47 This non-monotonic evolution emphasizes the importance of the atmospheric teleconnection  
48 between the two poles, which should be carefully considered to understand the polar climate.

49

50

## 51 **1. Introduction**

52           The increasing discharge of freshwater into the Southern Ocean (SO) from the  
53 Antarctic ice melt is one of the undeniable observed evidences and expected consequences of  
54 global warming. Recent satellite data indicate that Antarctic mass loss has increased sharply  
55 over the past 40 years (e.g., Rignot et al., 2019; Shepherd et al., 2018), and this trend is  
56 projected to continue in the next century (DeConto & Pollard, 2016; Hansen et al., 2016).  
57 The mass redistribution has been largely highlighted because it will contribute not only to the  
58 global sea level rise (Hanna et al., 2020) but also to a substantial response of the regional  
59 climate system associated with distinct structures of the SO (e.g., Bintanja et al., 2013). The  
60 ocean circulation surrounding Antarctica is characterized by a cold surface layer and a warm  
61 circumpolar deep water (CDW). As meltwater flows into the salty ocean, the low density  
62 further reduces ocean mixing, thereby inhibiting CDW upwelling (Fogwill et al., 2015), even  
63 though the horizontal gradient of ocean temperature and salinity under ice shelf could induce  
64 small-scale mixing and horizontal intrusion (Na et al., 2023). The CDW isolation modulates  
65 the biogeochemical properties of the SO (Bronse laer et al., 2020; Oh et al., 2022) and leads to  
66 increased sea-ice extent and decreased SO surface temperature (Park & Latif, 2019; Pauling  
67 et al., 2016).

68           Even local changes in extratropical regions can have noticeable effects in other  
69 regions: the tropics (Kang et al., 2020; Shin et al., 2021) and even the opposite extratropics  
70 (Cabr e et al., 2017; England et al., 2020; Shin & Kang, 2021). The meltwater-induced  
71 cooling is a representative example of such a global teleconnection, causing a northward shift  
72 of the Intertropical Convergence Zone (ITCZ)—a narrow band of rainfall near the equator—  
73 and global-wide cooling (Bakker & Prange, 2018; Bronse laer et al., 2018). This cooling  
74 pattern is accompanied by local cooling minima in the East Asia and the Subpolar Northern  
75 Atlantic (SPNA). The former has been proposed to be explained by the atmospheric Rossby  
76 wave teleconnection mechanism (Oh et al., 2020). The latter, the so-called cooling hole, is  
77 generally associated with the strengthening of the Atlantic Meridional Overturning  
78 Circulation (AMOC) (e.g., Buckley & Marshall, 2016; Keil et al., 2020), which suggests that  
79 the freshwater injection into the Southern Ocean eventually leads to a positive AMOC  
80 response (Li et al., 2023; Weaver et al., 2003). Furthermore, it is suggested that this will help  
81 to delay the AMOC collapse and its associated impacts (Sinet et al., 2023; Wunderling et al.,

82 2021). Therefore, the Antarctic meltwater has been widely emphasized for its potential role in  
83 mitigating both gradual and abrupt climate change.

84 While much attention has been paid to the impacts of Antarctic meltwater, less  
85 attention has been paid to its temporal evolution. It may be acceptable to pay less attention,  
86 given the slow time scale of ocean adjustment. However, the interplay between the  
87 atmospheric and the oceanic pathways could be of great importance in formulating climate  
88 responses on different time scales. For example, the Arctic sea-ice loss could lead to  
89 dramatically different impacts between longer multidecadal and on shorter decadal time  
90 scales (Liu & Fedorov, 2019). They showed that considerable time is required for the slow  
91 AMOC response to overcome the global atmospheric teleconnection induced by sea-ice loss,  
92 ultimately resulting in split climate patterns with respect to the time scale. Given that  
93 Antarctic meltwater input could lead to AMOC responses and also to atmospheric Rossby  
94 wave teleconnection, it is natural and reasonable to investigate the potential role of the  
95 Antarctic meltwater forcing in the AMOC and regional climate variations across various time  
96 scales.

97 The primary purpose of this study is accordingly to investigate the impact of  
98 Antarctic meltwater input on the AMOC and its temporal evolution. We conduct a series of  
99 experiments to identify the impact of meltwater input. Our findings reveal that an interplay  
100 between the atmospheric and oceanic pathways that can result in a non-monotonic response  
101 of the AMOC to the Antarctic meltwater input. This non-monotonic response emphasizes the  
102 connection between the two polar regions in regulating climate response to external forcing.

103

## 104 **2. Model and experiment**

105 In this study, we employ a fully coupled model, CM2.1, developed at the  
106 Geophysical Fluid Dynamics Laboratory (GFDL) (Delworth et al., 2006). The atmosphere  
107 and land models have a nominal 2° horizontal resolution, and the ocean and ice models have  
108 a nominal 1° horizontal resolution. We start with a 2000-year control simulation (CTL) at an  
109 atmospheric carbon dioxide concentration of 353 ppm, representing the 1990 level. The first  
110 1,000 years are discarded as a spin-up, and the last 1,000 years are used for as initial  
111 conditions for forced ensemble experiments. The MW\_off experiment is forced solely by an

112 atmospheric CO<sub>2</sub> that increases at a rate of 1% yr<sup>-1</sup> for 70 years and is then stayed with  
113 doubled CO<sub>2</sub> concentration (706 ppm). The MW<sub>on</sub> experiment is forced by both the same  
114 radiative forcing and an idealized Antarctic meltwater input. The meltwater discharge is  
115 introduced at the surface, assuming that it results from ice-sheet/shelf melting. The meltwater  
116 forcing is time-invariant 0.2 Sv freshwater discharge, equivalent to a sea level rise of 1.6 cm  
117 per year. This is expected amount around the year 2050 under representative concentration  
118 pathway 8.5 scenarios (DeConto & Pollard, 2016), and its distribution is proportional to the  
119 climatological runoff of Antarctica into the Southern Ocean. Hence, the most of meltwater is  
120 concentrated around West Antarctica following the recent observations (Rignot et al., 2019;  
121 Shepherd et al., 2018). The difference between the two experiments indicates the impact of  
122 Antarctic meltwater, denoted as  $\delta$ .

123 Both forced experiments are conducted with 12 ensemble members, each integrated  
124 from every 50 years of the control experiments. The statistical significance of meltwater  
125 impacts,  $\delta$ , is measured by a bootstrap analysis that calculates the 95% confidence level  
126 between the 25th and 975th values among randomly generated 1,000 bootstrap samples. Note  
127 that this set of experiments shares a general design with previous studies investigating  
128 Antarctic meltwater impacts (Oh et al., 2022; Park & Latif, 2019).

129

### 130 **3. Result**

131 The impact of Antarctic meltwater on global climate is shown in Figure 1. Doubling  
132 CO<sub>2</sub> warms the global mean surface temperature by 1.6 K without meltwater input (red in  
133 Figure 1a). As previous studies suggested, the Antarctic meltwater reduces surface warming  
134 (blue in Figure 1a). The global cooling effect peaks at year 31, reaching -0.41 K, and then  
135 gradually weakens (Figure 1b). Note that this gradual weakening of the cooling effect is  
136 commonly reported in studies using time-invariant meltwater input (e.g., Park and Latif 2019;  
137 Oh et al. 2020), regarded as the compensation of subsurface warming with limited heat  
138 reservoir of the deep ocean (Martin et al., 2013; Zhang & Delworth, 2016). Nevertheless, the  
139 meltwater input always reduces global mean surface warming.

140 Meltwater-induced cooling is strongest in the SO following geographic adjacency,  
141 especially near West Antarctica (Figure 1e). This cooling extends to the entire Southern

142 Hemisphere and tropics, even in the Arctic (e.g., Bronselaer et al., 2018). In addition, the  
143 tropical precipitation shows a distinct pattern: a zonal-mean northward shift and a weakening  
144 of walker circulation (green-brown contour in Figure 1e). The former has been relatively  
145 well-established since the early 2000s, first noticed by paleoclimate proxies and modeling  
146 experiments (e.g., Chiang & Bitz, 2005; Peterson et al., 2000). Theoretical studies suggest  
147 that the zonal-mean precipitation is shifted to the north which reduces the meltwater-induced  
148 interhemispheric energy asymmetry (e.g., Kang et al., 2018a). The latter is more complex as  
149 not only the governing dynamics but also either forcing structure or model dependency would  
150 modulate tropical precipitation patterns. However, it is worth noting that this anomalous  
151 precipitation pattern to the Antarctic meltwater forcing is consistently shown in other models  
152 (see Figure 2 in Bronselaer et al., 2018; Figure 2 in Oh et al., 2020).

153 In climate models, the AMOC is generally expected to weaken under global warming  
154 (e.g., Levang & Schmitt, 2020; Reintges et al., 2017), and the Antarctic meltwater is expected  
155 to counteract the weakening. Consistently, in our experiments, the meltwater input tends to  
156 strengthen the AMOC after 30 years, when the cooling peaks, mitigating the impacts of  
157 global warming. However, the AMOC fluctuation significantly depends on the time scale  
158 (Figures 1c-d) as well as the temperature minimum at the SPNA (Figure S1a). In particular,  
159 prior to this period, the meltwater unexpectedly weakens the AMOC (Figure 1d). Considering  
160 that the temperature response generally retains its pattern with respect to the time (Figure  
161 S1b), the AMOC response to the meltwater-induced cooling shows not a simple linear but a  
162 non-monotonic relationship, which is counterintuitive to the large inertia of the ocean  
163 circulation that would be expected to produce a more gradual response to the perennial  
164 cooling.

165 To understand this non-monotonic response in detail, we look at the periods before  
166 and after the AMOC transition, referred to as weak and strong periods (orange and gray  
167 shading in Figure 1). We first note that, although the AMOC responses are opposite, the  
168 zonal-mean ocean circulation response in the SO and tropics is somewhat similar (Figures 1f-  
169 g). In the southern extratropics, the freshwater input reduces the formation of Antarctic  
170 Bottom Water, while the cold surface intensifies a meridional temperature gradient and  
171 westerly winds, accompanied by enhanced Deacon cell (Park & Latif, 2019). In the tropics,  
172 the northward ITCZ shift indicates a weakening of the northern Hadley cell, and vice versa.  
173 Since the atmospheric and oceanic circulation are mechanically coupled through surface wind

174 stress, subtropical cell responses mirror the changes occurring on the Hadley cell (Held,  
175 2001), compensating meltwater-induced interhemispheric asymmetry (e.g., Green &  
176 Marshall, 2017; Kang et al., 2018b; Schneider, 2017). Only in the northern extratropics the  
177 oceanic circulation is dependent on the time scale. During the strong period, the AMOC  
178 generally strengthens (Figure 1g), which is consistent with previous studies reporting the  
179 long-term response of the AMOC to meltwater input and/or the surface cooling hole  
180 (Bronse laer et al., 2018; Oh et al., 2020; Park & Latif, 2019). However, just a few years after  
181 the freshwater forcing, the AMOC experiences a significant weakening. Note that it closely  
182 resembles the response of the AMOC to freshwater input from Greenland, the antipode of  
183 Antarctica (Figure 1f; Figures 6a-c in Li et al., 2023).

184 Focusing on the weak period, we examine the temporal evolution of upper-ocean  
185 density in the Atlantic basin (Figure 2). The density responses are most pronounced above  
186 500 m, suggesting that upper-level stratification plays an important role in regulating the  
187 AMOC (Figure S2). The Hovmöller diagram shows that the Atlantic upper-ocean density  
188 suddenly decreases at northern high-latitude at the beginning of weak period, which  
189 corresponds to the weakening of the AMOC (Figures 2a and S2a). The density reduction is  
190 solely pronounced in the deep convection region of the AMOC, the Labrador Sea (Figure 2b),  
191 where even small perturbations can induce large AMOC responses (e.g., Stocker & Wright,  
192 1991). Salinity plays a dominant role in driving the density decrease. Although cold  
193 temperature has the potential to increase the density (Figure 2g-h), it cannot overcome  
194 surface freshening (Figure 2d-e). Note that these regions have been proposed to be diluted by  
195 freshwater fluxes from Greenland (Gillard et al., 2016), which partially explains the  
196 aforementioned similarity with the results of the Greenland freshwater hosing experiment (Li  
197 et al., 2023).

198 The local stratification is eventually terminated by Atlantic-wide cooling. Although  
199 local freshening continues to weaken the AMOC (Figures 2d-f), thermally-driven density  
200 anomalies emerge from low-latitudes and propagate northward through the upper ocean,  
201 gradually overcoming the stratification at the deep convection region (Figures 2a-c and S2).  
202 Temperature anomalies evolve along the Atlantic water pathway (Figure S3), implying the  
203 importance of climatological upper-ocean circulation in regulating SPNA convection  
204 (Piecuch et al., 2017). Within a few decades, the whole North Atlantic upper ocean, as well as  
205 the SPNA, is eventually de-stratified by thermal contraction. It is followed by a strengthening

206 of the AMOC and a cessation of the weak periods. This time scale is comparable to previous  
207 results, showing that it takes a few decades for tropical salinity to spread throughout the  
208 North Atlantic (see Figure S12 in Hu & Fedorov, 2019). We note that the near-surface (0-5 m)  
209 density evolution is almost consistent with that in the upper ocean (Figure S4). Taken  
210 together, the density profiles clearly indicate that some rapid response to the Antarctic  
211 meltwater input abruptly dilutes the deep convection regions near Greenland, leading to an  
212 unrecognized weakening of the AMOC.

213 Atmospheric processes are intuitively the most likely candidate for abrupt salinity  
214 reduction, not only because of their fast time scale but also because of the importance of  
215 large-scale atmospheric circulation in regulating salinity (e.g., Durack et al., 2012). Thermal  
216 forcing imposed in the SO could influence tropical climate through the lower troposphere,  
217 leading to changes in the tropical hydrological cycle within a few years (Kim et al., 2022). As  
218 the tropical convection is modulated, the resulting Gill-type response could rapidly perturb  
219 the extratropical climate via the wave train propagating poleward and eastward (Hoskins &  
220 Karoly, 1981). Hence, we examine the precipitation and 300hPa streamfunction response at  
221 the onset of the weak period (Figure 3a). Suppressed convection is detected in the western  
222 Pacific warm pool region, which excites upper-level cyclonic flow and the wave energy  
223 continues to propagate northeastward across North America. The associated wave activity  
224 flux (WAF) suggests that the wave propagation eventually gives rise to the anticyclonic  
225 circulation over Greenland, which projects onto a negative NAO pattern. The teleconnection  
226 is quite similar to that shown in previous studies which suggest a strong positive correlation  
227 between western Pacific convection and NAO response (e.g., Geng et al., 2023; Huntingford  
228 et al., 2014; Scaife et al., 2017). Note that the wave train is consistently shown in the boreal  
229 winter (DJF), when both the Rossby wave teleconnection and the SPNA deep convection are  
230 dominant (Figure S5). The NAO is known to modulate the AMOC intensity through the  
231 surface buoyancy response in the deep convection regions (e.g., Kim et al., 2023; Medhaug  
232 et al., 2012). In alignment with this, the presence of an anticyclone over Greenland  
233 corresponds to a weakening of the surface westerly winds over the SPNA, resulting in a  
234 significant reduction of regional evaporation (Figure 3b). While regional precipitation shows  
235 a slight decrease with the anticyclone (not shown), the downward water flux at the surface–  
236 precipitation minus evaporation (P-E)–shows a significant decrease mainly due to the

237 evaporation reduction. This decrease explains the salinity drop at the onset of weak periods,  
238 inducing feeble convection at the Labrador Sea (Figure 2a,e).

239 We further analyzed the 1000-year control experiment to consolidate the tropical-  
240 induced salinity decrease over the SPNA. In order to link the high-latitude circulation  
241 response to tropical convection, we first regress the interannual precipitation variability in  
242 control simulation against the meltwater-induced tropical precipitation pattern (dashed box in  
243 Figure 3a), so that the regression coefficient could serve as a quantifiable indicator of the  
244 spatial correspondence between the precipitation variability and the meltwater-induced  
245 response. Then, based on the regression coefficient, we extract the variability that reflects the  
246 tropical precipitation response to the Antarctic meltwater and accompanied outcomes, such as  
247 Rossby wave train, again by regression analysis (Figures 3c-d). Note that the reconstructed  
248 precipitation pattern is not perfectly consistent with that forced by the Antarctic meltwater  
249 (contour in Figure 3c), as the former mostly reflects zonal redistribution of diabatic heating,  
250 while the latter represents a combination of meridional shift and zonal redistribution.  
251 Nevertheless, the western Pacific diabatic cooling induces a similar wave train that  
252 propagates northeastward to the SPNA, leading to anticyclonic circulation over Greenland  
253 (Figure 3c). In line with the change at the onset of the weak period, we also observe a  
254 subsequent decrease in both surface wind speed and evaporation (Figure 3d). Considering the  
255 Labrador and Irminger Sea, the correlation between the forced and regression patterns stands  
256 at a strong 0.82 for evaporation and 0.71 for surface wind speed (dashed box in Figure 3b).  
257 The spatial similarity underscores the crucial role of atmospheric teleconnection in regulating  
258 the climate of the North Atlantic.

259

#### 260 **4. Summary and Discussion**

261 In this study, we investigate the impact of Antarctic meltwater on the AMOC with  
262 particular interest in its temporal evolution. Previous studies have shown that Antarctic  
263 meltwater induces global cooling, and both the atmosphere and the ocean circulation adjust to  
264 it, such as the northward shift of the ITCZ and the strengthening of the Deacon cell  
265 (Bronseleer et al., 2018; Park & Latif, 2019). However, our study suggests that while the  
266 AMOC strengthening is stably detected after 30 years of simulation, it is unexpectedly  
267 weakened during the initial period by the Antarctic meltwater discharge, which makes a non-

268 monotonic AMOC response to global cooling (Figure 4). The non-monotonic response is  
269 attributed to the differing timescales of atmospheric and oceanic teleconnections. The SO  
270 cooling could affect the tropical climate within a few years through near-surface propagation,  
271 resulting in convection redistribution (Kang et al., 2023; Kim et al., 2022). Then, the  
272 suppressed convection immediately triggers an upper-level cyclonic flow, which initiates  
273 Rossby wave propagation to the extratropics. Before the Atlantic gyre system brings tropical  
274 cooling into the SPNA convection region that is followed by the AMOC strengthening, the  
275 wave-induced anticyclone over Greenland, which is a polarity of the negative NAO pattern,  
276 weakens the surface westerlies, evaporation, and the strength of the AMOC. Therefore, the  
277 non-monotonic response of the AMOC, consistently shown as a tug-of-war in the SPNA  
278 upper-ocean density, is the result of competing influences between atmospheric  
279 teleconnection, which induces rapid and regional freshening, and oceanic propagation, which  
280 results in slow but strong thermal stratification.

281         Although the amount of freshwater is plausible under global warming scenarios  
282 (DeConto & Pollard, 2016), employing an abrupt and time-invariant freshwater forcing in our  
283 experiments may exaggerate the temporal evolution of the meltwater impacts under global  
284 warming. For example, the suggested non-monotonicity is not anticipated from the southern  
285 high-latitude warming that slowly emerges after we succeed in reducing atmospheric CO<sub>2</sub>  
286 concentrations (Kug et al., 2021). Rather, this non-monotonicity is more likely to occur when  
287 sudden and disastrous changes happen, which aligns with the growing concern about various  
288 tipping elements (McKay et al., 2022) and their interaction, referred to as tipping cascading  
289 (Wunderling et al., 2023). Our current understanding of these cascading impacts is still  
290 limited to conceptual and idealized models. For example, conceptual models that consider the  
291 oceanic transport alone propose the abrupt meltwater discharge from the West Antarctic Ice  
292 Sheet (WAIS) as a potential stabilizing factor for the AMOC (Sinet et al., 2023). However,  
293 our findings point out a new dimension that the WAIS could also provoke AMOC  
294 destabilization through the atmospheric pole-to-pole teleconnection. We note that there are  
295 alternative pathways that could link SPNA and tropics such as Indo-Pacific Ocean (e.g., Hu  
296 & Fedorov, 2020; Orihuela-Pinto et al., 2023) and aforementioned NAO-AMOC relationship  
297 is known to depend on oceanic mean state (Kim et al., 2023). Considering the intricate nature  
298 of climate systems, further studies are warranted to carefully investigate the meltwater  
299 impacts on both gradual and abrupt climate change by employing a more realistic

300 configuration. The primary purpose of this study, however, is to highlight the potential of  
301 non-monotonic AMOC response by the interplay between atmosphere and ocean pathways.

302

303 **Acknowledgments**

304 This research was supported by Korea Institute of Marine Science & Technology Promotion  
305 (KIMST) funded by the Ministry of Oceans and Fisheries (RS-2023-00256677; PM23020)  
306 and by the National Research Foundation of Korea (NRF) grant funded by the Korean  
307 government (NRF-2022R1A3B1077622)

308

309 **Data Availability Statement**

310 The processed data of the simulations used for this study is available on Zenodo  
311 (<https://zenodo.org/records/10056446>)

312

313 **Reference**

- 314 Armstrong McKay, D. I., Staal, A., Abrams, J. F., Winkelmann, R., Sakschewski, B., Loriani,  
 315 S., et al. (2022). Exceeding 1.5°C global warming could trigger multiple climate  
 316 tipping points. *Science*, 377(6611), eabn7950.  
 317 <https://doi.org/10.1126/science.abn7950>
- 318 Bakker, P., & Prange, M. (2018). Response of the Intertropical Convergence Zone to  
 319 Antarctic Ice Sheet Melt. *Geophysical Research Letters*, 45(16), 8673–8680.  
 320 <https://doi.org/10.1029/2018GL078659>
- 321 Bintanja, R., van Oldenborgh, G. J., Drijfhout, S. S., Wouters, B., & Katsman, C. A. (2013).  
 322 Important role for ocean warming and increased ice-shelf melt in Antarctic sea-ice  
 323 expansion. *Nature Geoscience*, 6(5), 376–379. <https://doi.org/10.1038/ngeo1767>
- 324 Bronselaer, B., Winton, M., Griffies, S. M., Hurlin, W. J., Rodgers, K. B., Sergienko, O. V., et  
 325 al. (2018). Change in future climate due to Antarctic meltwater. *Nature*, 564(7734),  
 326 53–58. <https://doi.org/10.1038/s41586-018-0712-z>
- 327 Bronselaer, B., Russell, J. L., Winton, M., Williams, N. L., Key, R. M., Dunne, J. P., et al.  
 328 (2020). Importance of wind and meltwater for observed chemical and physical  
 329 changes in the Southern Ocean. *Nature Geoscience*, 13(1), 35–42.  
 330 <https://doi.org/10.1038/s41561-019-0502-8>
- 331 Buckley, M. W., & Marshall, J. (2016). Observations, inferences, and mechanisms of the  
 332 Atlantic Meridional Overturning Circulation: A review. *Reviews of Geophysics*, 54(1),  
 333 5–63. <https://doi.org/10.1002/2015RG000493>
- 334 Cabré, A., Marinov, I., & Gnanadesikan, A. (2017). Global Atmospheric Teleconnections and  
 335 Multidecadal Climate Oscillations Driven by Southern Ocean Convection. *Journal of*  
 336 *Climate*, 30(20), 8107–8126. <https://doi.org/10.1175/JCLI-D-16-0741.1>
- 337 Chiang, J. C. H., & Bitz, C. M. (2005). Influence of high latitude ice cover on the marine  
 338 Intertropical Convergence Zone. *Climate Dynamics*, 25(5), 477–496.  
 339 <https://doi.org/10.1007/s00382-005-0040-5>
- 340 DeConto, R. M., & Pollard, D. (2016). Contribution of Antarctica to past and future sea-level  
 341 rise. *Nature*, 531(7596), 591–597. <https://doi.org/10.1038/nature17145>
- 342 Delworth, T. L., Broccoli, A. J., Rosati, A., Stouffer, R. J., Balaji, V., Beesley, J. A., et al.  
 343 (2006). GFDL’s CM2 Global Coupled Climate Models. Part I: Formulation and  
 344 Simulation Characteristics. *Journal of Climate*, 19(5), 643–674.  
 345 <https://doi.org/10.1175/JCLI3629.1>
- 346 Durack, P. J., Wijffels, S. E., & Matear, R. J. (2012). Ocean Salinities Reveal Strong Global  
 347 Water Cycle Intensification During 1950 to 2000. *Science*, 336(6080), 455–458.  
 348 <https://doi.org/10.1126/science.1212222>
- 349 England, M. R., Polvani, L. M., & Sun, L. (2020). Robust Arctic warming caused by  
 350 projected Antarctic sea ice loss. *Environmental Research Letters*, 15(10), 104005.  
 351 <https://doi.org/10.1088/1748-9326/abaada>
- 352 Fogwill, C. J., Phipps, S. J., Turney, C. S. M., & Golledge, N. R. (2015). Sensitivity of the  
 353 Southern Ocean to enhanced regional Antarctic ice sheet meltwater input. *Earth’s*

- 354 *Future*, 3(10), 317–329. <https://doi.org/10.1002/2015EF000306>
- 355 Geng, X., Zhao, J., & Kug, J.-S. (2023). ENSO-driven abrupt phase shift in North Atlantic  
356 oscillation in early January. *Npj Climate and Atmospheric Science*, 6(1), 1–8.  
357 <https://doi.org/10.1038/s41612-023-00414-2>
- 358 Gillard, L. C., Hu, X., Myers, P. G., & Bamber, J. L. (2016). Meltwater pathways from  
359 marine terminating glaciers of the Greenland ice sheet. *Geophysical Research Letters*,  
360 43(20), 10,873–10,882. <https://doi.org/10.1002/2016GL070969>
- 361 Green, B., & Marshall, J. (2017). Coupling of Trade Winds with Ocean Circulation Damps  
362 ITCZ Shifts. *Journal of Climate*, 30(12), 4395–4411. [https://doi.org/10.1175/JCLI-D-](https://doi.org/10.1175/JCLI-D-16-0818.1)  
363 16-0818.1
- 364 Hanna, E., Pattyn, F., Navarro, F., Favier, V., Goelzer, H., van den Broeke, M. R., et al.  
365 (2020). Mass balance of the ice sheets and glaciers – Progress since AR5 and  
366 challenges. *Earth-Science Reviews*, 201, 102976.  
367 <https://doi.org/10.1016/j.earscirev.2019.102976>
- 368 Hansen, J., Sato, M., Hearty, P., Ruedy, R., Kelley, M., Masson-Delmotte, V., et al. (2016).  
369 Ice melt, sea level rise and superstorms: evidence from paleoclimate data, climate  
370 modeling, and modern observations that 2 °C global warming could be dangerous.  
371 *Atmospheric Chemistry and Physics*, 16(6), 3761–3812. [https://doi.org/10.5194/acp-](https://doi.org/10.5194/acp-16-3761-2016)  
372 16-3761-2016
- 373 Held, I. M. (2001). The Partitioning of the Poleward Energy Transport between the Tropical  
374 Ocean and Atmosphere. *Journal of the Atmospheric Sciences*, 58(8), 943–948.  
375 [https://doi.org/10.1175/1520-0469\(2001\)058<0943:TPOTPE>2.0.CO;2](https://doi.org/10.1175/1520-0469(2001)058<0943:TPOTPE>2.0.CO;2)
- 376 Hu, S., & Fedorov, A. V. (2019). Indian Ocean warming can strengthen the Atlantic  
377 meridional overturning circulation. *Nature Climate Change*, 9(10), 747–751.  
378 <https://doi.org/10.1038/s41558-019-0566-x>
- 379 Hu, S., & Fedorov, A. V. (2020). Indian Ocean warming as a driver of the North Atlantic  
380 warming hole. *Nature Communications*, 11(1), 4785. [https://doi.org/10.1038/s41467-](https://doi.org/10.1038/s41467-020-18522-5)  
381 020-18522-5
- 382 Huntingford, C., Marsh, T., Scaife, A. A., Kendon, E. J., Hannaford, J., Kay, A. L., et al.  
383 (2014). Potential influences on the United Kingdom’s floods of winter 2013/14.  
384 *Nature Climate Change*, 4(9), 769–777. <https://doi.org/10.1038/nclimate2314>
- 385 Kang, S. M., Shin, Y., & Xie, S.-P. (2018). Extratropical forcing and tropical rainfall  
386 distribution: energetics framework and ocean Ekman advection. *Npj Climate and*  
387 *Atmospheric Science*, 1(1), 1–10. <https://doi.org/10.1038/s41612-017-0004-6>
- 388 Kang, S. M., Shin, Y., & Codron, F. (2018). The partitioning of poleward energy transport  
389 response between the atmosphere and Ekman flux to prescribed surface forcing in a  
390 simplified GCM. *Geoscience Letters*, 5(1), 22. [https://doi.org/10.1186/s40562-018-](https://doi.org/10.1186/s40562-018-0124-9)  
391 0124-9
- 392 Kang, S. M., Xie, S.-P., Shin, Y., Kim, H., Hwang, Y.-T., Stuecker, M. F., et al. (2020).  
393 Walker circulation response to extratropical radiative forcing. *Science Advances*,  
394 6(47), eabd3021. <https://doi.org/10.1126/sciadv.abd3021>
- 395 Kang, S. M., Shin, Y., Kim, H., Xie, S.-P., & Hu, S. (2023). Disentangling the mechanisms of

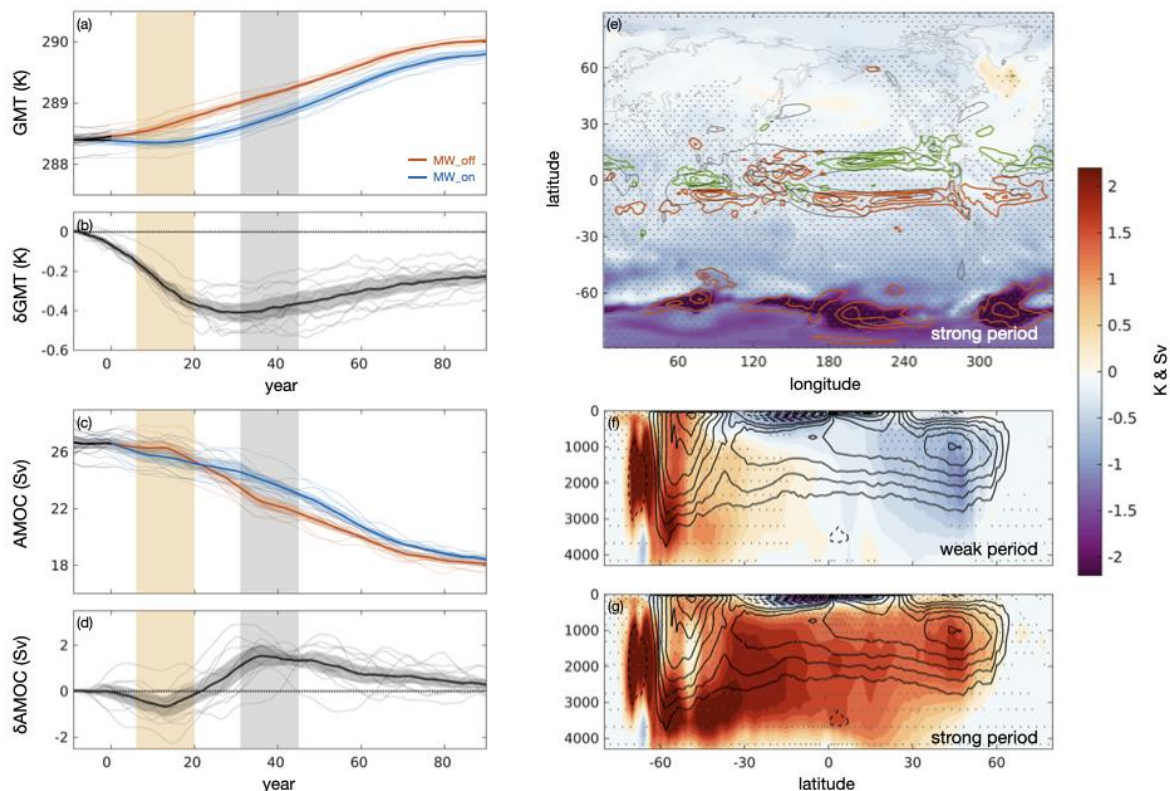
- 396 equatorial Pacific climate change. *Science Advances*, 9(19), eadf5059.  
397 <https://doi.org/10.1126/sciadv.adf5059>
- 398 Keil, P., Mauritsen, T., Jungclauss, J., Hedemann, C., Olonscheck, D., & Ghosh, R. (2020).  
399 Multiple drivers of the North Atlantic warming hole. *Nature Climate Change*, 10(7),  
400 667–671. <https://doi.org/10.1038/s41558-020-0819-8>
- 401 Kim, H., Kang, S. M., Kay, J. E., & Xie, S.-P. (2022). Subtropical clouds key to Southern  
402 Ocean teleconnections to the tropical Pacific. *Proceedings of the National Academy of*  
403 *Sciences*, 119(34), e2200514119. <https://doi.org/10.1073/pnas.2200514119>
- 404 Kim, H.-J., An, S.-I., Park, J.-H., Sung, M.-K., Kim, D., Choi, Y., & Kim, J.-S. (2023). North  
405 Atlantic Oscillation impact on the Atlantic Meridional Overturning Circulation shaped  
406 by the mean state. *Npj Climate and Atmospheric Science*, 6(1), 1–13.  
407 <https://doi.org/10.1038/s41612-023-00354-x>
- 408 Kug, J.-S., Oh, J.-H., An, S.-I., Yeh, S.-W., Min, S.-K., Son, S.-W., et al. (2021). Hysteresis of  
409 the intertropical convergence zone to CO<sub>2</sub> forcing. *Nature Climate Change*, 1–7.  
410 <https://doi.org/10.1038/s41558-021-01211-6>
- 411 Levang, S. J., & Schmitt, R. W. (2020). What Causes the AMOC to Weaken in CMIP5?  
412 *Journal of Climate*, 33(4), 1535–1545. <https://doi.org/10.1175/JCLI-D-19-0547.1>
- 413 Li, Q., Marshall, J., Rye, C. D., Romanou, A., Rind, D., & Kelley, M. (2023). Global Climate  
414 Impacts of Greenland and Antarctic Meltwater: A Comparative Study. *Journal of*  
415 *Climate*, 1(aop), 1–40. <https://doi.org/10.1175/JCLI-D-22-0433.1>
- 416 Liu, W., & Fedorov, A. V. (2019). Global Impacts of Arctic Sea Ice Loss Mediated by the  
417 Atlantic Meridional Overturning Circulation. *Geophysical Research Letters*, 46(2),  
418 944–952. <https://doi.org/10.1029/2018GL080602>
- 419 Martin, T., Park, W., & Latif, M. (2013). Multi-centennial variability controlled by Southern  
420 Ocean convection in the Kiel Climate Model. *Climate Dynamics*, 40(7), 2005–2022.  
421 <https://doi.org/10.1007/s00382-012-1586-7>
- 422 Medhaug, I., Langehaug, H. R., Eldevik, T., Furevik, T., & Bentsen, M. (2012). Mechanisms  
423 for decadal scale variability in a simulated Atlantic meridional overturning  
424 circulation. *Climate Dynamics*, 39(1), 77–93. [https://doi.org/10.1007/s00382-011-](https://doi.org/10.1007/s00382-011-1124-z)  
425 [1124-z](https://doi.org/10.1007/s00382-011-1124-z)
- 426 Na, J. S., Davis, P. E. D., Kim, B., Jin, E. K., & Lee, W. S. (2023). Ice Shelf Water Structure  
427 Beneath the Larsen C Ice Shelf in Antarctica. *Geophysical Research Letters*, 50(19),  
428 e2023GL104088. <https://doi.org/10.1029/2023GL104088>
- 429 Oh, J.-H., Park, W., Lim, H.-G., Noh, K. M., Jin, E. K., & Kug, J.-S. (2020). Impact of  
430 Antarctic Meltwater Forcing on East Asian Climate Under Greenhouse Warming.  
431 *Geophysical Research Letters*, 47(21), e2020GL089951.  
432 <https://doi.org/10.1029/2020GL089951>
- 433 Oh, J.-H., Noh, K. M., Lim, H.-G., Jin, E. K., Jun, S.-Y., & Kug, J.-S. (2022). Antarctic  
434 meltwater-induced dynamical changes in phytoplankton in the Southern Ocean.  
435 *Environmental Research Letters*, 17(2), 024022. [https://doi.org/10.1088/1748-](https://doi.org/10.1088/1748-9326/ac444e)  
436 [9326/ac444e](https://doi.org/10.1088/1748-9326/ac444e)
- 437 Orihuela-Pinto, B., Santoso, A., England, M. H., & Taschetto, A. S. (2023). Coupled

- 438        Feedbacks From the Tropical Pacific to the Atlantic Meridional Overturning  
439        Circulation. *Geophysical Research Letters*, 50(20), e2023GL103250.  
440        <https://doi.org/10.1029/2023GL103250>
- 441    Park, W., & Latif, M. (2019). Ensemble global warming simulations with idealized Antarctic  
442        meltwater input. *Climate Dynamics*, 52(5), 3223–3239.  
443        <https://doi.org/10.1007/s00382-018-4319-8>
- 444    Pauling, A. G., Bitz, C. M., Smith, I. J., & Langhorne, P. J. (2016). The Response of the  
445        Southern Ocean and Antarctic Sea Ice to Freshwater from Ice Shelves in an Earth  
446        System Model. *Journal of Climate*, 29(5), 1655–1672. [https://doi.org/10.1175/JCLI-](https://doi.org/10.1175/JCLI-D-15-0501.1)  
447        [D-15-0501.1](https://doi.org/10.1175/JCLI-D-15-0501.1)
- 448    Peterson, L. C., Haug, G. H., Hughen, K. A., & Röhl, U. (2000). Rapid Changes in the  
449        Hydrologic Cycle of the Tropical Atlantic During the Last Glacial. *Science*,  
450        290(5498), 1947–1951. <https://doi.org/10.1126/science.290.5498.1947>
- 451    Piecuch, C. G., Ponte, R. M., Little, C. M., Buckley, M. W., & Fukumori, I. (2017).  
452        Mechanisms underlying recent decadal changes in subpolar North Atlantic Ocean heat  
453        content. *Journal of Geophysical Research: Oceans*, 122(9), 7181–7197.  
454        <https://doi.org/10.1002/2017JC012845>
- 455    Reintges, A., Martin, T., Latif, M., & Keenlyside, N. S. (2017). Uncertainty in twenty-first  
456        century projections of the Atlantic Meridional Overturning Circulation in CMIP3 and  
457        CMIP5 models. *Climate Dynamics*, 49(5), 1495–1511.  
458        <https://doi.org/10.1007/s00382-016-3180-x>
- 459    Rignot, E., Mouginot, J., Scheuchl, B., van den Broeke, M., van Wessem, M. J., &  
460        Morlighem, M. (2019). Four decades of Antarctic Ice Sheet mass balance from 1979–  
461        2017. *Proceedings of the National Academy of Sciences*, 116(4), 1095–1103.  
462        <https://doi.org/10.1073/pnas.1812883116>
- 463    Scaife, A. A., Comer, R. E., Dunstone, N. J., Knight, J. R., Smith, D. M., MacLachlan, C., et  
464        al. (2017). Tropical rainfall, Rossby waves and regional winter climate predictions.  
465        *Quarterly Journal of the Royal Meteorological Society*, 143(702), 1–11.  
466        <https://doi.org/10.1002/qj.2910>
- 467    Schneider, T. (2017). Feedback of Atmosphere-Ocean Coupling on Shifts of the Intertropical  
468        Convergence Zone. *Geophysical Research Letters*, 44(22), 11,644–11,653.  
469        <https://doi.org/10.1002/2017GL075817>
- 470    Shepherd, A., Fricker, H. A., & Farrell, S. L. (2018). Trends and connections across the  
471        Antarctic cryosphere. *Nature*, 558(7709), 223–232. [https://doi.org/10.1038/s41586-](https://doi.org/10.1038/s41586-018-0171-6)  
472        [018-0171-6](https://doi.org/10.1038/s41586-018-0171-6)
- 473    Shin, Y., & Kang, S. M. (2021). How Does the High-Latitude Thermal Forcing in One  
474        Hemisphere Affect the Other Hemisphere? *Geophysical Research Letters*, 48(24),  
475        e2021GL095870. <https://doi.org/10.1029/2021GL095870>
- 476    Shin, Y., Kang, S. M., Takahashi, K., Stuecker, M. F., Hwang, Y.-T., & Kim, D. (2021).  
477        Evolution of the Tropical Response to Periodic Extratropical Thermal Forcing.  
478        *Journal of Climate*, 1(aop), 1–53. <https://doi.org/10.1175/JCLI-D-20-0493.1>
- 479    Sinet, S., von der Heydt, A. S., & Dijkstra, H. A. (2023). AMOC Stabilization Under the

- 480 Interaction With Tipping Polar Ice Sheets. *Geophysical Research Letters*, 50(2),  
481 e2022GL100305. <https://doi.org/10.1029/2022GL100305>
- 482 Stocker, T. F., & Wright, D. G. (1991). Rapid transitions of the ocean's deep circulation  
483 induced by changes in surface water fluxes. *Nature*, 351(6329), 729–732.  
484 <https://doi.org/10.1038/351729a0>
- 485 Weaver, A. J., Saenko, O. A., Clark, P. U., & Mitrovica, J. X. (2003). Meltwater Pulse 1A  
486 from Antarctica as a Trigger of the Bølling-Allerød Warm Interval. *Science*,  
487 299(5613), 1709–1713. <https://doi.org/10.1126/science.1081002>
- 488 Wunderling, N., Donges, J. F., Kurths, J., & Winkelmann, R. (2021). Interacting tipping  
489 elements increase risk of climate domino effects under global warming. *Earth System*  
490 *Dynamics*, 12(2), 601–619. <https://doi.org/10.5194/esd-12-601-2021>
- 491 Wunderling, N., von der Heydt, A., Aksenov, Y., Barker, S., Bastiaansen, R., Brovkin, V., et  
492 al. (2023). Climate tipping point interactions and cascades: A review. *EGUsphere*, 1–  
493 45. <https://doi.org/10.5194/egusphere-2023-1576>
- 494 Zhang, L., & Delworth, T. L. (2016). Impact of the Antarctic bottom water formation on the  
495 Weddell Gyre and its northward propagation characteristics in GFDL CM2.1 model.  
496 *Journal of Geophysical Research: Oceans*, 121(8), 5825–5846.  
497 <https://doi.org/10.1002/2016JC011790>  
498

499 **Figure list**

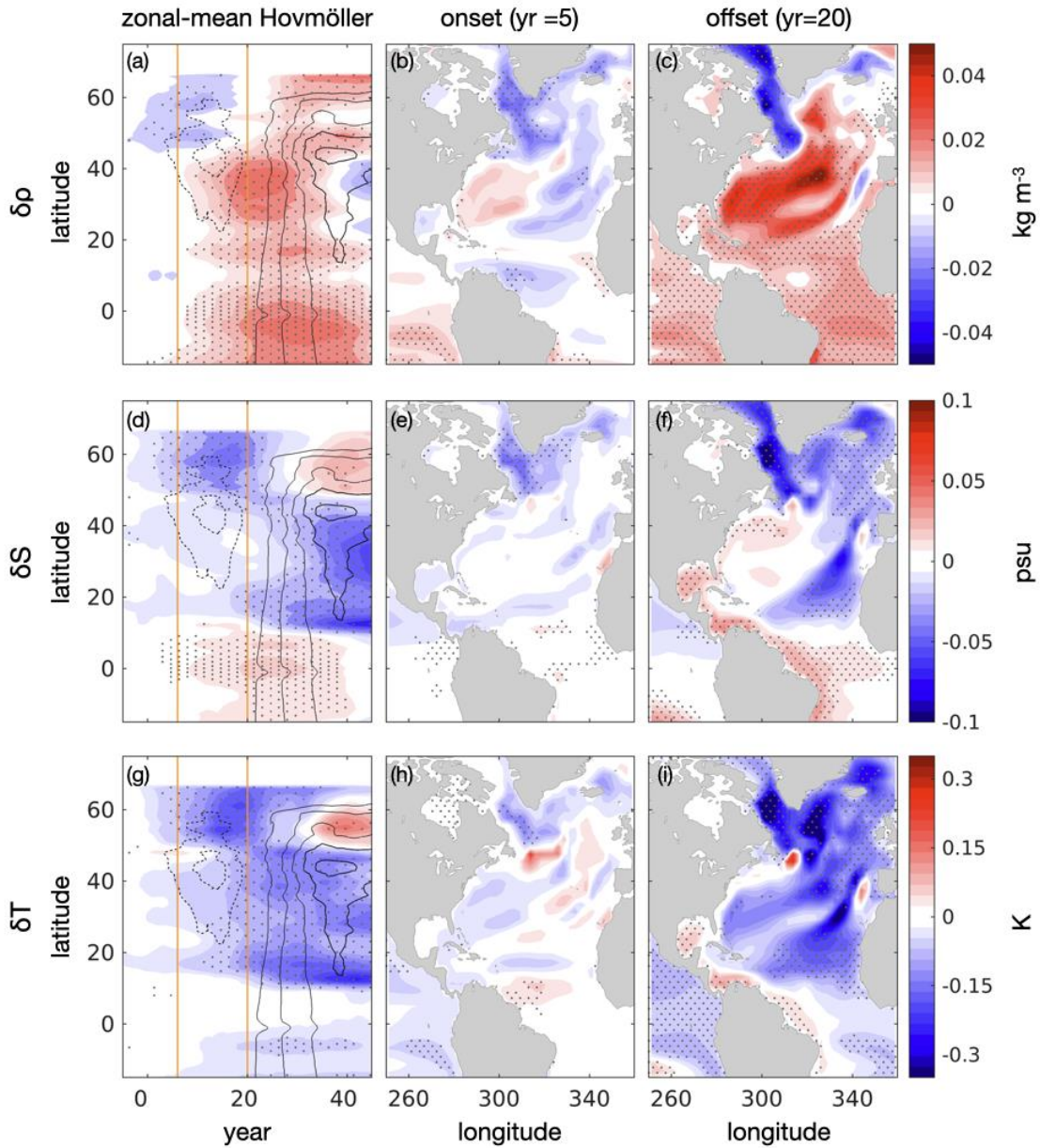
500



501

502 **Figure 1.** Time series of (a) global mean surface temperature. Red is the ensemble with CO<sub>2</sub>  
 503 doubling only (MW\_off), while blue is the ensemble with additional Antarctic meltwater  
 504 discharge (MW\_on). (b) Meltwater-induced response in global mean surface temperature  
 505 (i.e., blue-red). (c,d) Same time series as (a,b), but for the AMOC index, measuring the  
 506 maximum meridional stream function at 45°N. Every time series is smoothed by 21-yr  
 507 running average. Each ensemble members are shown as a thin line, with its mean as a thick  
 508 line. Shading indicates the statistical range at the 95% confidence level. Gray vertical shading  
 509 indicates a strong period, while orange shading indicates a weak period. (e) Meltwater-  
 510 induced surface temperature (shading) and precipitation (green-brown contour; interval =  
 511 0.13 mm day<sup>-1</sup>) anomalies at the strong period. Black solid contour is climatological  
 512 precipitation (interval = 5 mm day<sup>-1</sup>). (f) Response of the meridional overturning circulation  
 513 (shading) at the weak period and (g) at the strong period. Climatological MOC is shown in  
 514 solid-dashed contour (interval = 3 Sv). Red shading and solid contour indicate clockwise

515 circulation and vice versa. Dotted area indicates statistical significance at the 95% confidence  
 516 level.

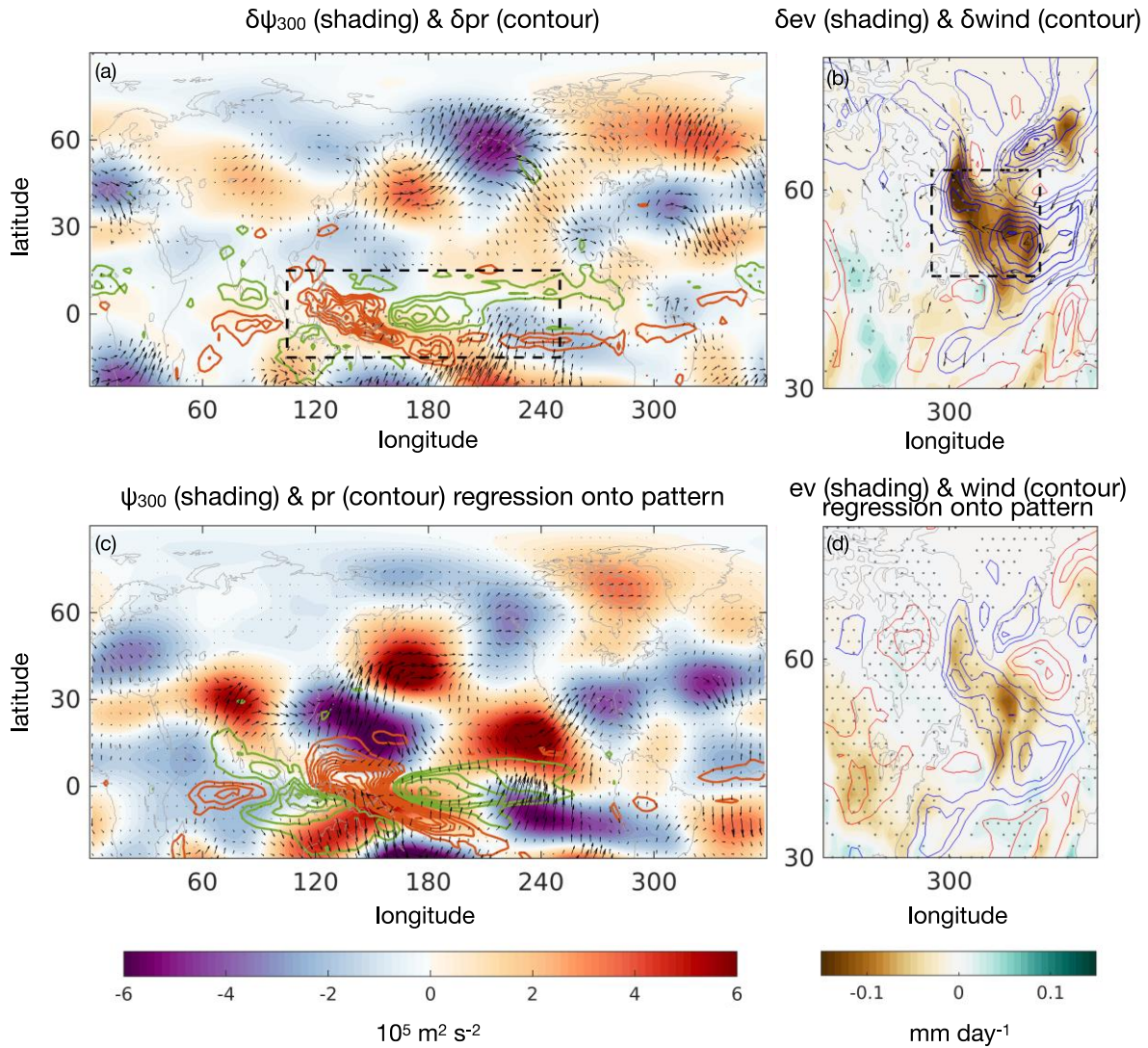


517

518 **Figure 2.** (left) Atlantic zonal-mean Hovmöller diagram of upper-level (0-500m) (a) density,  
 519 (g) salinity, and (g) temperature. The meridional stream function at 1000 m is shown as a  
 520 solid-dashed contour (interval = 0.3 Sv). The onset and offset of the weak period are shown  
 521 as orange lines. All variables are 21-year running averaged. (middle) Anomalous map for  
 522 corresponding variable at onset and (right) offset. Dotted area indicates statistical significance  
 523 at the 95% confidence level.



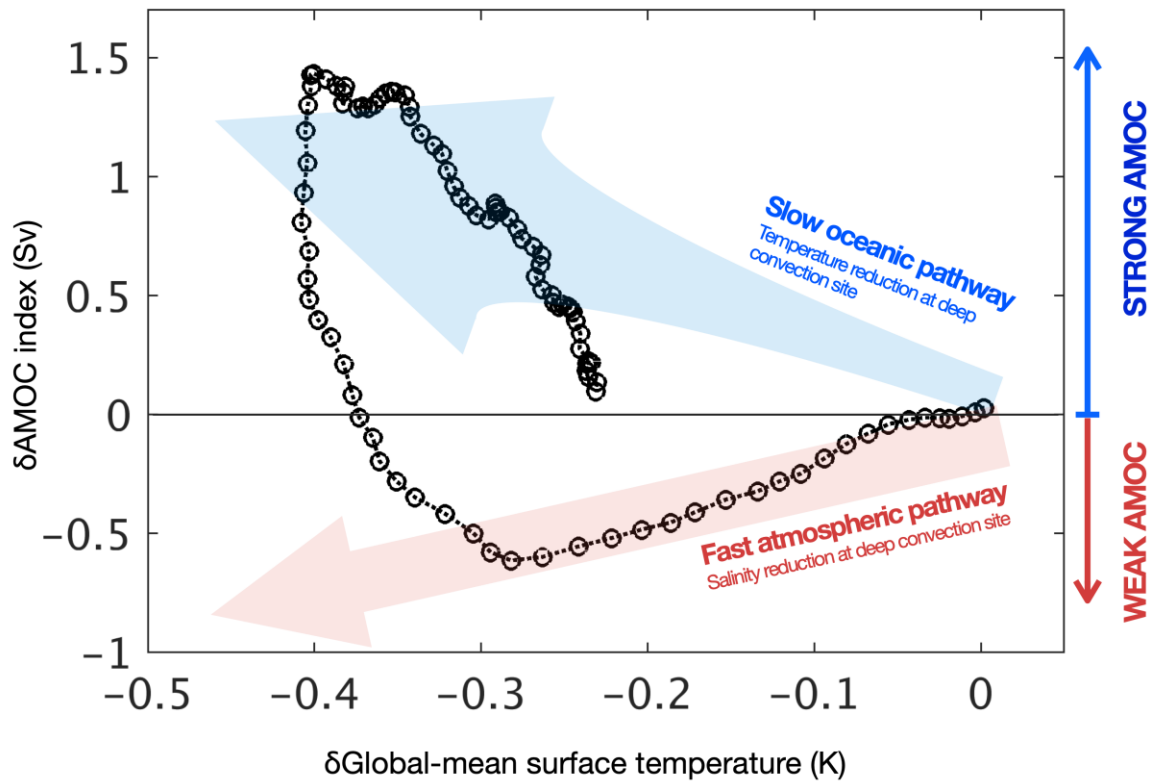
525



526

527 **Figure 3.** (a) Annual-mean stream function at 300 hPa (shading), precipitation (green-brown  
 528 contour; interval =  $0.1 \text{ mm day}^{-1}$ ), and wave activity flux (quiver) anomalies, and (b)  
 529 evaporation (shading), surface wind speed (red-blue contour; interval =  $0.02 \text{ m s}^{-1}$ ), and 10 m  
 530 wind (quiver) anomalies to the Antarctic meltwater input at the onset of weak period (yr 5 to  
 531 12). (c,d) Same maps as (a,b) but for the regression coefficient of each variable on the  
 532 anomalous precipitation pattern. Dotted regions are statistically significant at the 95%  
 533 confidence level. The dashed box in (a) indicates the anomalous precipitation pattern for  
 534 regression analysis, and that in (b) indicates the Labrador and Irminger Seas.

535



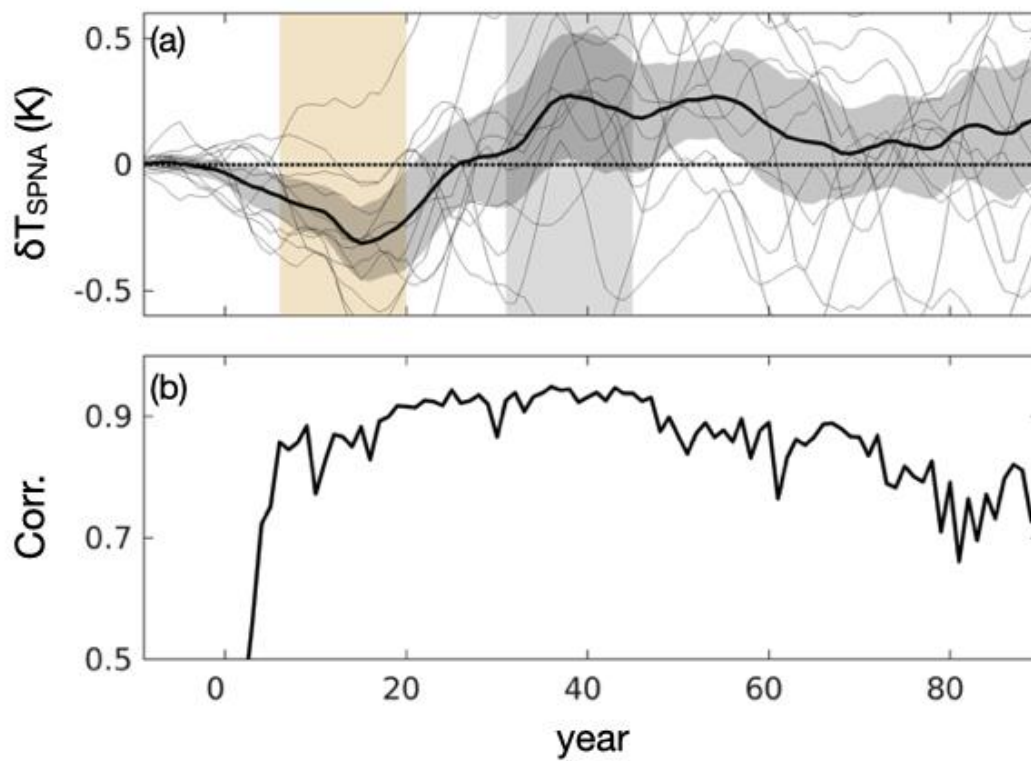
536

537 **Figure 4.** Meltwater-induced AMOC anomalies with respect to the global-mean surface  
 538 cooling. Each circle indicates 21-year running-mean annual-mean value. Although the global-  
 539 mean temperature decreases by the meltwater hosing, the AMOC response is muted for the  
 540 first few years corresponding to the time lag between Southern Ocean cooling and tropical  
 541 response. Then, the AMOC response is not following the intuitive strengthening, but  
 542 weakening which is driven by fast atmospheric pathway. As time goes by, slow but strong  
 543 ocean pathway reaches the deep convection region, the AMOC exhibits abrupt transition  
 544 under relatively consistent global-mean cooling.

545

546

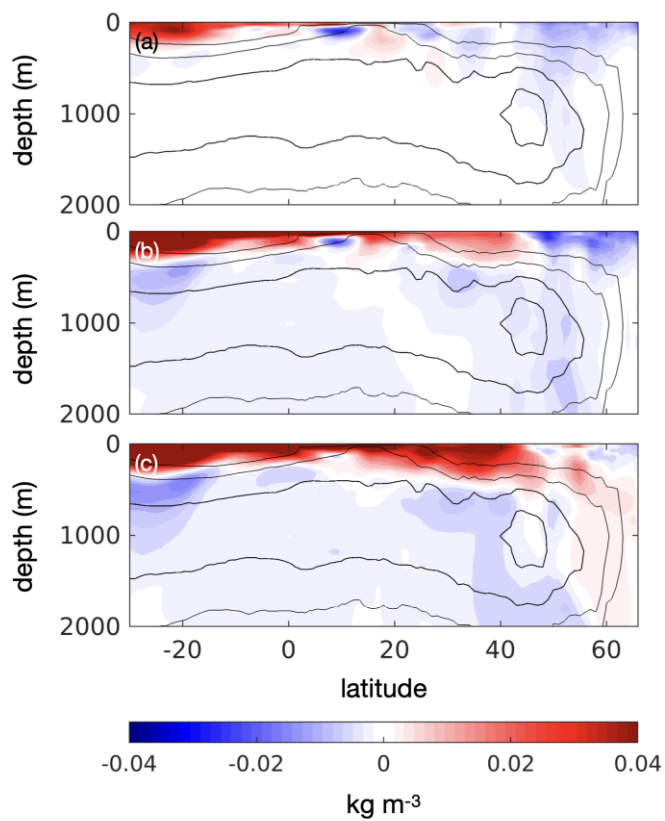
547



548

549 **Figure S1.** (a) Same time series as Figure 1b but for SPNA surface temperature ( $50^{\circ}\text{N}\sim 60^{\circ}\text{N}$ ,  
550  $300^{\circ}\text{E}\sim 320^{\circ}\text{E}$ ). (b) Time series of pattern correlation coefficient between  $\delta T_{\text{S}}$  at each year and that of  
551 strong period, shown in Fig. 1e.

552

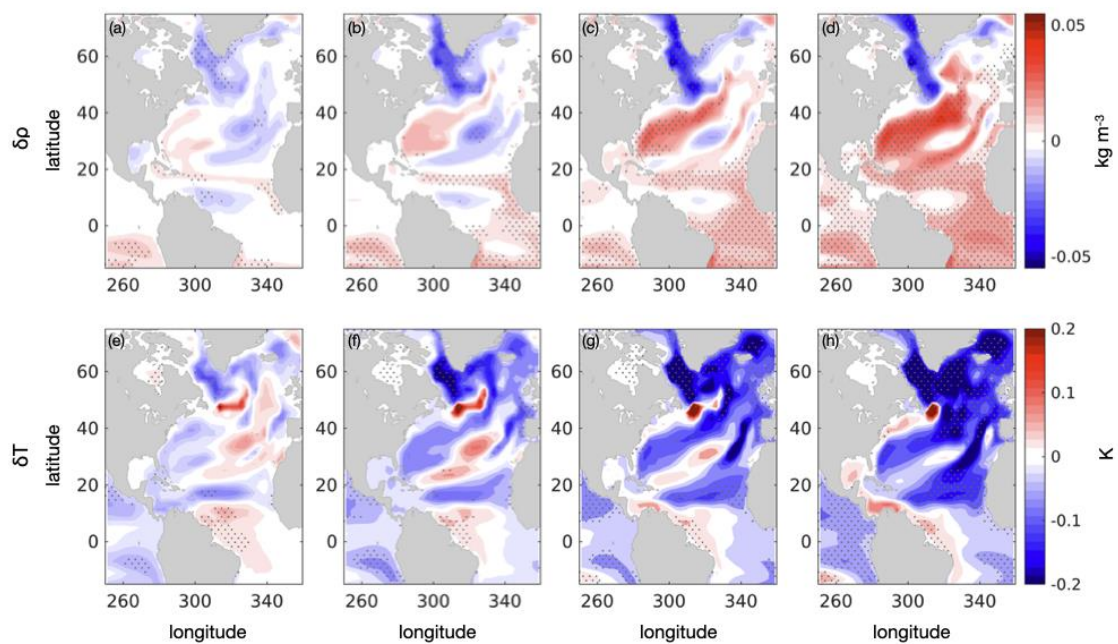


553

554 **Figure S2.** (a) Atlantic depth-latitude profile of the anomalous density response to the Antarctic  
555 meltwater at the onset, (b) middle, (c) offset of the weak period. Climatological mean meridional  
556 stream function is shown in solid contour (interval = 4 Sv).

557

558

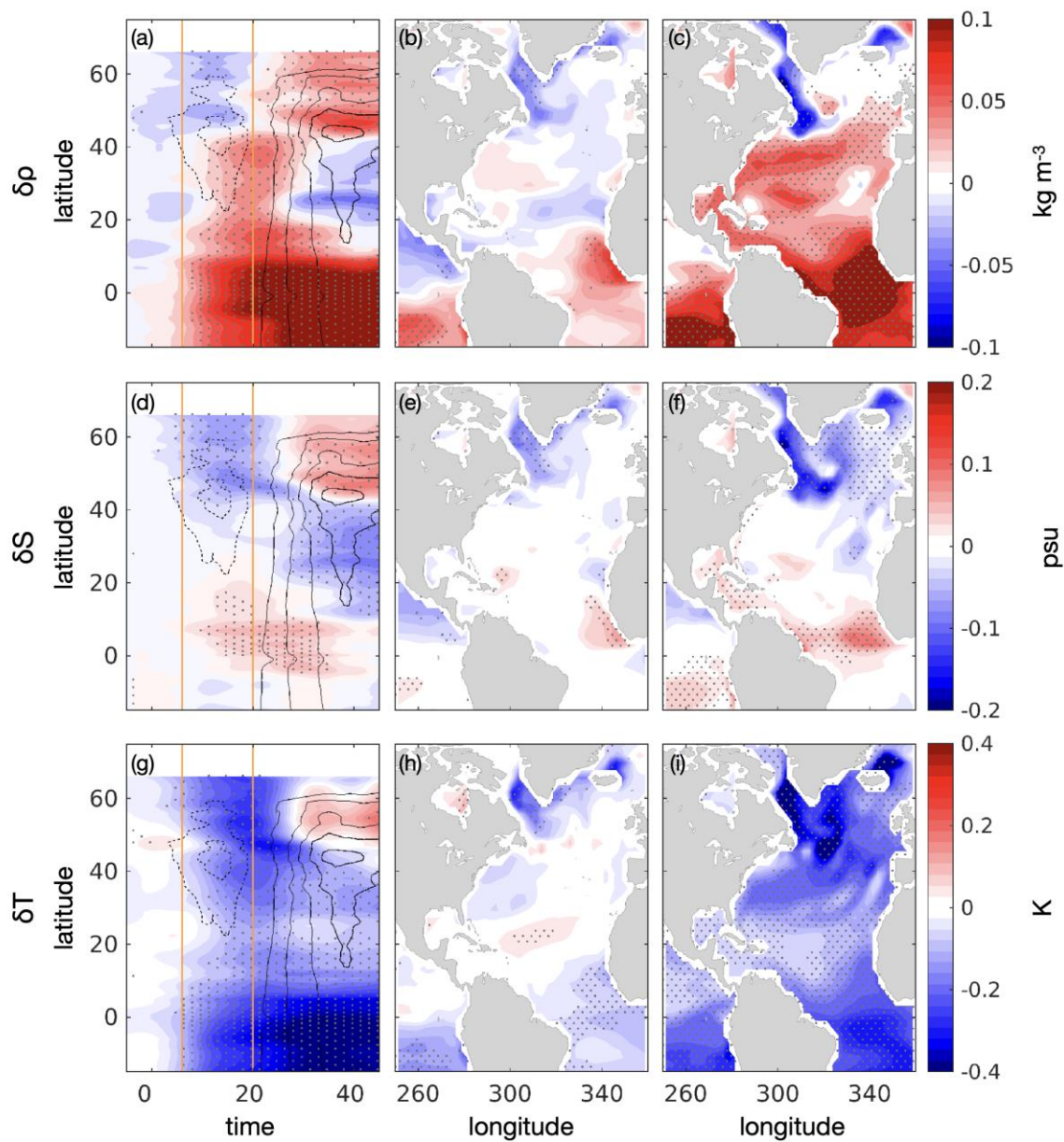


559

560 **Figure S3.** Anomalous map for upper-level (0-500m) density and temperature (a,e) of the  
561 onset of the weak period and (b-d,f-h) every 4 year from thereafter.

562

563

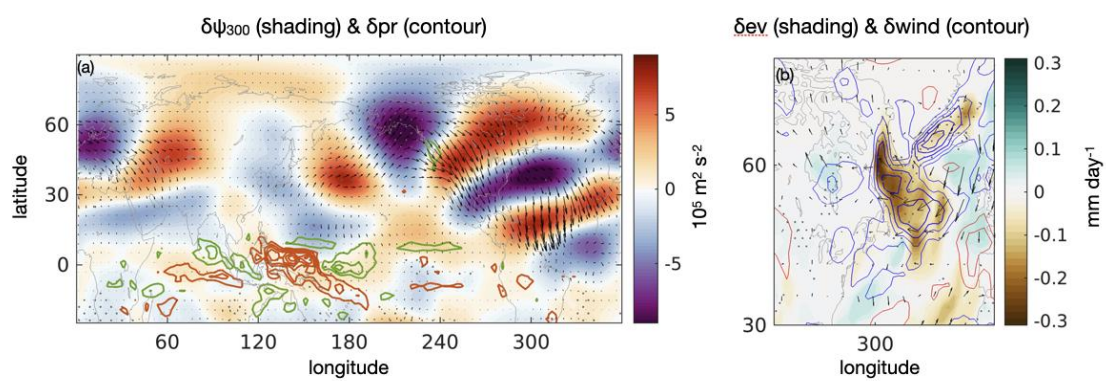


564

565

566 **Figure S4.** Same as Figure 2 but for surface layer.

567



568

569 **Figure S5.** Same as Figure 3a and b but for the boreal winter (DJF).

570



*[Geophysical Research Letters]*

Supporting Information for

## **Non-monotonic responses of Atlantic Meridional Overturning Circulation to Antarctic meltwater forcing**

Yechul Shin<sup>1</sup>, Xin Geng<sup>1,2</sup>, Ji-Hoon Oh<sup>1</sup>, Kyung-Min Noh<sup>1</sup>, Emilia Kyung Jin<sup>3</sup>,  
and Jong-Seong Kug<sup>1\*</sup>

<sup>1</sup>Division of Environmental Science and Engineering, Pohang University of Science and  
Technology (POSTECH), Pohang, Republic of Korea

<sup>2</sup>CIC-FEMD/ILCEC, Key Laboratory of Meteorological Disaster of Ministry of  
Education (KLME), Nanjing University of Information Science and Technology,  
Nanjing, China.

<sup>3</sup>Institute Korea Polar Research Institute (KOPRI), Incheon, Republic of Korea

### **Contents of this file**

Figures S1 to S5

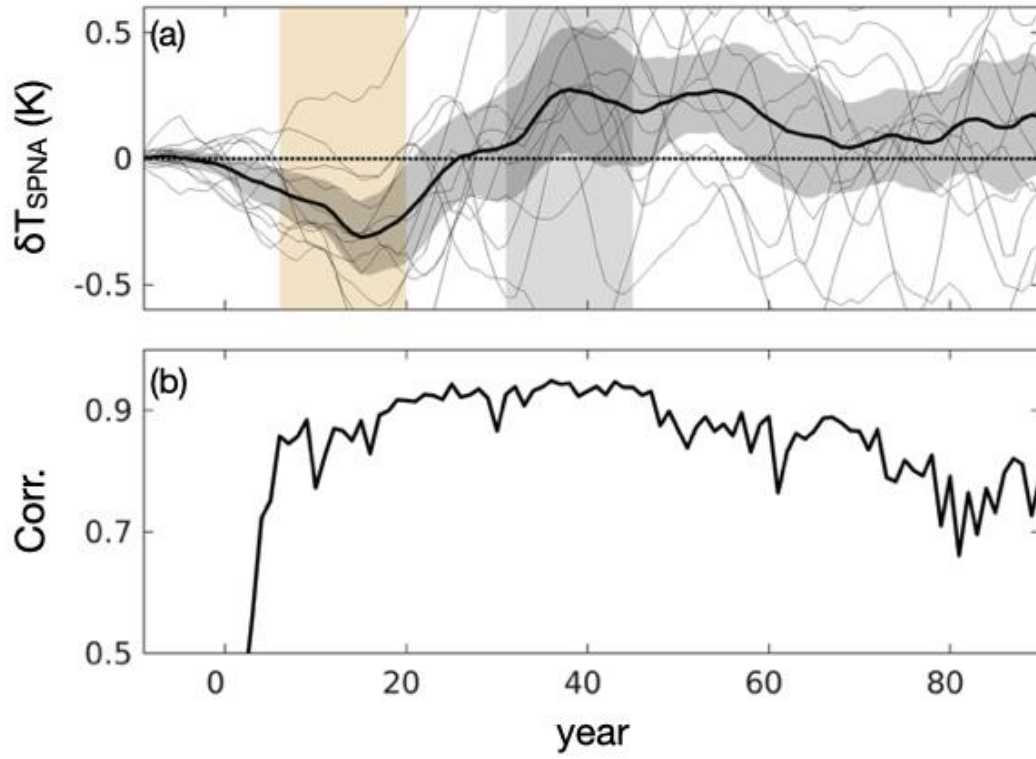


**Figure S1.** (a) Same time series as Figure 1b but for SPNA surface temperature (50°N~60°N, 300°E~320°E). (b) Time series of pattern correlation coefficient between  $\delta T_s$  at each year and that of strong period, shown in Fig. 1e.

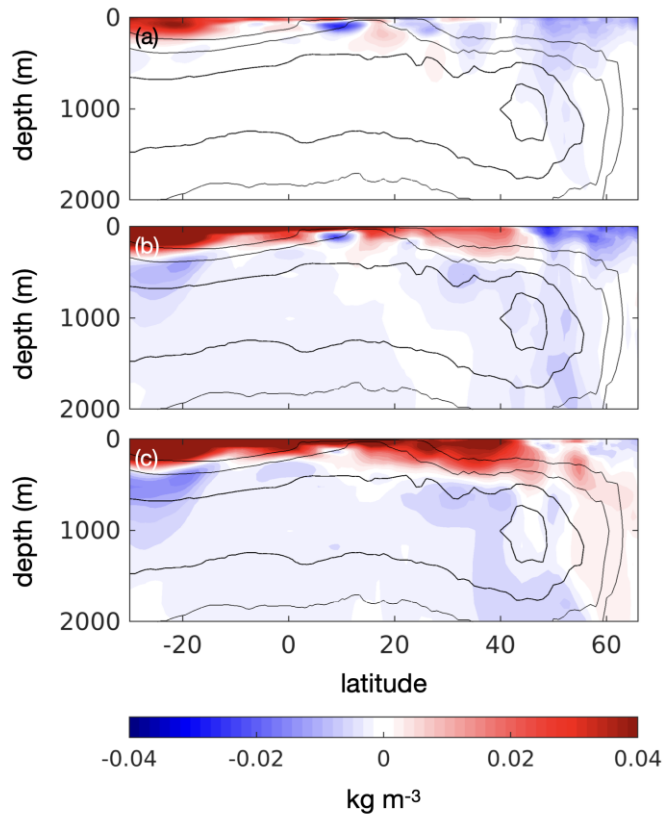


**Figure S2.** (a) Atlantic depth-latitude profile of the anomalous density response to the Antarctic meltwater at the onset, (b) middle, (c) offset of the weak period. Climatological mean meridional stream function is shown in solid contour (interval = 4 Sv).

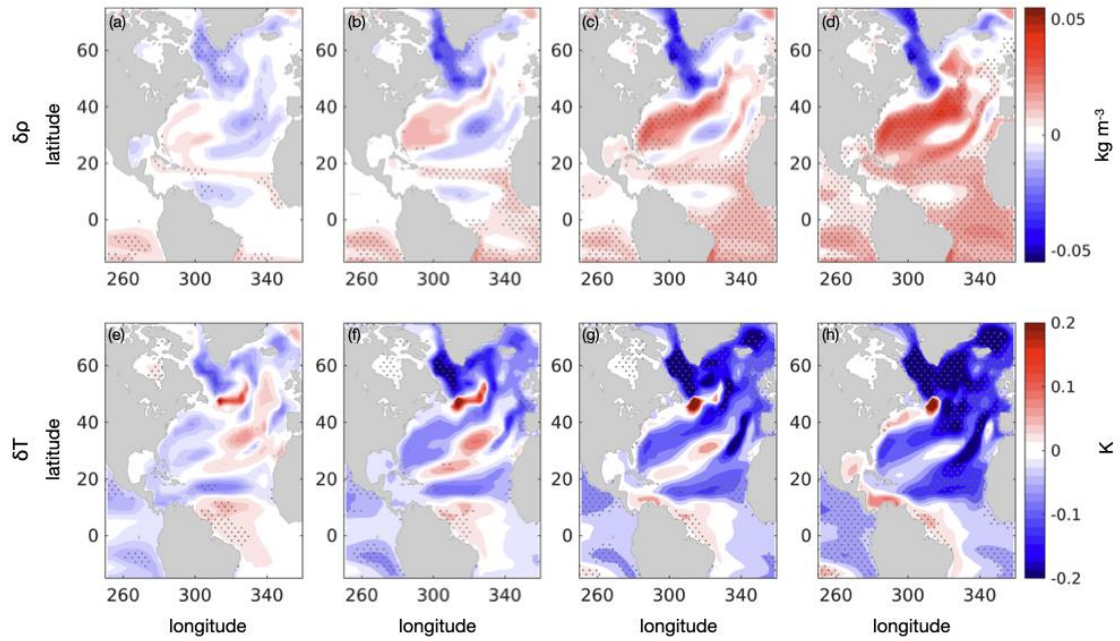


**Figure S3.** Anomalous map for upper-level (0-500m) density and temperature (a,e) of the onset of the weak period and (b-d,f-h) every 4 year from thereafter.

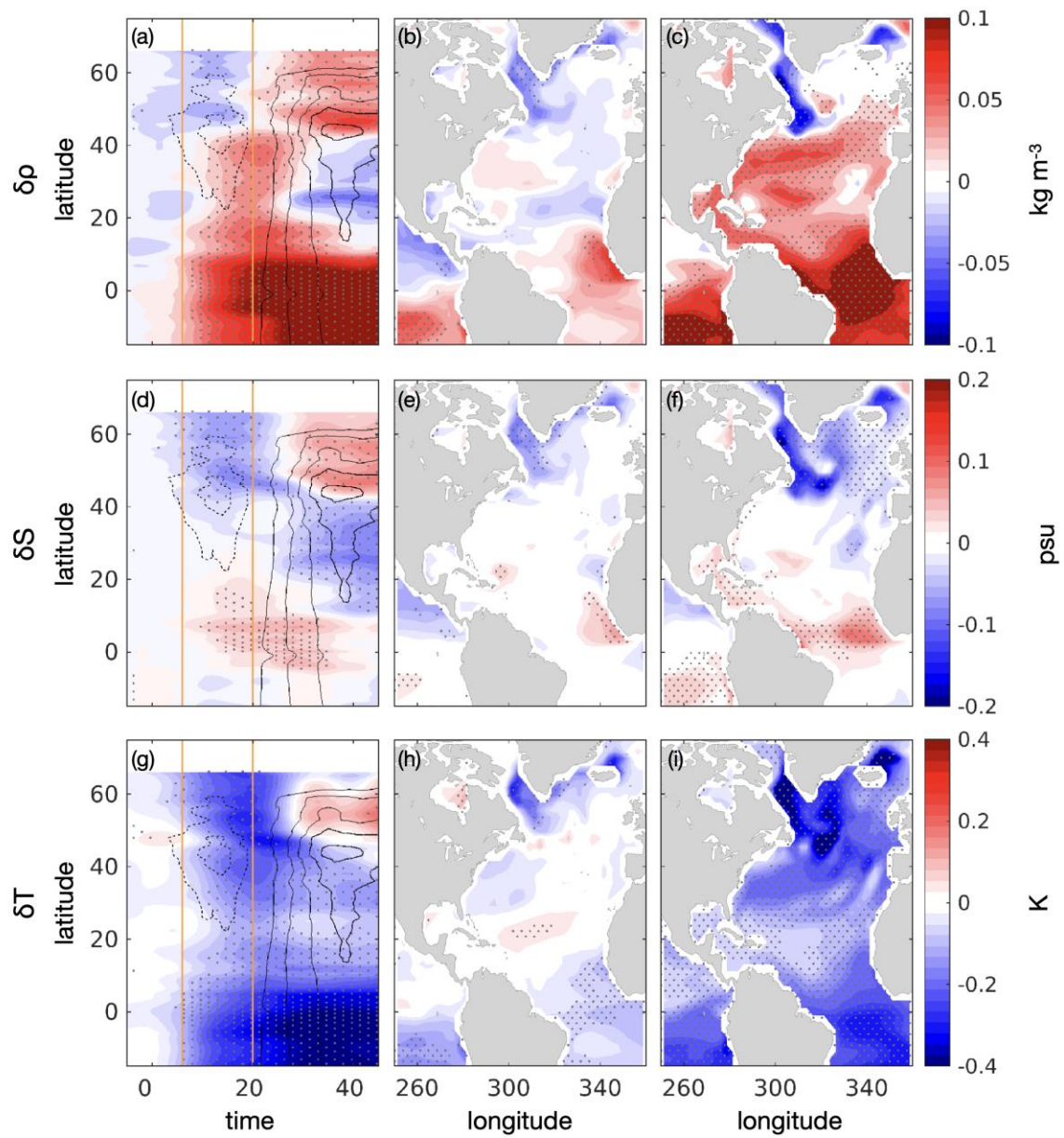


**Figure S4.** Same as Figure 2 but for the surface layer.

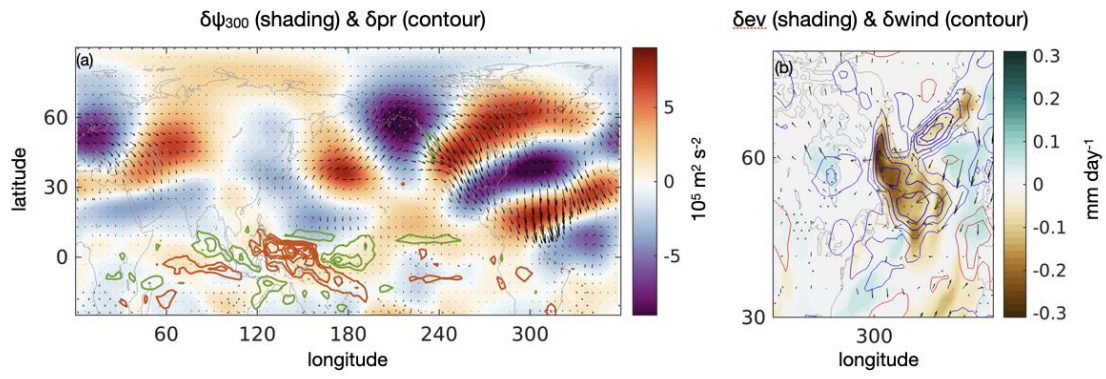


**Figure S5.** Same as Figure 3a and b but for the boreal winter (DJF).